ISSN 1674-1056
http://cpb.iphy.ac.cn
http://iopscience.iop.org/cpb
中国物理 B
Chinese Physics
中国物理 Chinese Physics B

Improvement of TE-polarized emission in type-Ⅱ InAlN-AlGaN/AlGaN quantum well

Yi Li(李毅), Youhua Zhu(朱友华), Meiyu Wang(王美玉), Honghai Deng(邓洪海), Haihong Yin(尹海宏)
Citation: Chin. Phys. B . 2019, 28(9): 097801 . **doi:** 10.1088/1674-1056/28/9/097801
Journal homepage: http://cpb.iphy.ac.cn; http://iopscience.iop.org/cpb

What follows is a list of articles you may be interested in

Non-perturbative multiphoton excitation studies in an excitonic coupled quantum well system using high-intensity THz laser fields

Monica Gambhir, Vinod Prasad
Chin. Phys. B . 2019, 28(8): 087803 . **doi:** 10.1088/1674-1056/28/8/087803

Progress in quantum well and quantum cascade infrared photodetectors in SITP

Xiaohao Zhou(周孝好), Ning Li(李宁), Wei Lu(陆卫)
Chin. Phys. B . 2019, 28(2): 027801 . **doi:** 10.1088/1674-1056/28/2/027801

Optimizing effective phase modulation in coupled double quantum well Mach-Zehnder modulators

Guang-Hui Wang(王光辉), Jin-Ke Zhang(张金珂)
Chin. Phys. B . 2018, 27(2): 027801 . **doi:** 10.1088/1674-1056/27/2/027801

Analysis of localization effect in blue-violet light emitting InGaN/GaN multiple quantum wells with different well widths

Xiang Li(李翔), De-Gang Zhao(赵德刚), De-Sheng Jiang(江德生), Jing Yang(杨静), Ping Chen(陈平), Zong-Shun Liu(刘宗顺), Jian-Jun Zhu(朱建军), Wei Liu(刘炜), Xiao-Guang He(何晓光), Xiao-Jing Li(李晓静), Feng Liang(梁锋), Jian-Ping Liu(刘建平), Li-Qun Zhang(张立群), Hui Yang(杨辉), Yuan-Tao Zhang(张源涛), Guo-Tong Du(杜国同), Heng Long(龙衡), Mo Li(李沫)
Chin. Phys. B . 2017, 26(1): 017805 . **doi:** 10.1088/1674-1056/26/1/017805

Direct observation of the carrier transport process in InGaN quantum wells with a pn-junction

Haiyan Wu(吴海燕), Ziguang Ma(马紫光), Yang Jiang(江洋), Lu Wang(王禄), Haojun Yang(杨浩军), Yangfeng Li(李阳锋), Peng Zuo(左朋), Haiqiang Jia(贾海强), Wenxin Wang(王文新), Junming Zhou(周钧铭), Wuming Liu(刘伍明), Hong Chen(陈弘)
Chin. Phys. B . 2016, 25(11): 117803 . **doi:** 10.1088/1674-1056/25/11/117803

Improvement of TE-polarized emission in type-II InAlN–AlGaN/AlGaN quantum well*

Yi Li(李毅), Youhua Zhu(朱友华)†, Meiyu Wang(王美玉), Honghai Deng(邓洪海), and Haihong Yin(尹海宏)

School of Information Science and Technology & Tongke School of Microelectronics, Nantong University, Nantong 226019, China

(Received 6 June 2019; revised manuscript received 7 July 2019; published online 7 August 2019)

The optical properties of the type-II lineup $In_xAl_{1-x}N$–$Al_{0.59}Ga_{0.41}N/Al_{0.74}Ga_{0.26}N$ quantum well (QW) structures with different In contents are investigated by using the six-by-six K–P method. The type-II lineup structures exhibit the larger product of Fermi–Dirac distribution functions of electron f_c^n and hole $(1-f_v^{Um})$ and the approximately equal transverse electric (TE) polarization optical matrix elements ($|M_x|^2$) for the c1–v1 transition. As a result, the peak intensity in the TE polarization spontaneous emission spectrum is improved by 47.45%–53.84% as compared to that of the conventional AlGaN QW structure. In addition, the type-II QW structure with $x \sim 0.17$ has the largest TE mode peak intensity in the investigated In-content range of 0.13–0.23. It can be attributed to the combined effect of $|M_x|^2$ and $f_c^n(1-f_v^{Um})$ for the c1–v1, c1–v2, and c1–v3 transitions.

Keywords: type-II lineup, quantum well, K-P method, transverse electric (TE) polarized emission

PACS: 78.66.Fd, 78.67.De, 78.67.–n, 78.67.Pt **DOI:** 10.1088/1674-1056/ab343a

1. Introduction

III-nitride deep-ultraviolet (DUV) light-emitting diodes (LEDs) have attracted more and more attention due to their potential applications such as the sterilization-medical use and illumination.[1] However, compared to the GaN-based blue LEDs, the DUV LEDs have much lower external quantum efficiencies due to the high dislocation density, the poor p-type doping, and the low light extraction efficiency.[2] In general, the structure design strategy can be employed to improve the performance of DUV LEDs.[3] For example, Hirayama *et al.* reported that the emission efficiency of DUV LEDs can be significantly enhanced by using the multi-quantum barrier (MQB) electron-blocking layer (EBL).[4] The improvement can be attributed to the increase of the electron injection efficiency. Liu *et al.* proposed an AlN-delta-GaN quantum well (QW) structure, which can improve the transverse electric (TE)-polarized surface emission.[2] For the AlGaN-based LEDs, it is well known that the transverse-magnetic (TM) polarized emission will become dominant with increasing the Al-content due to the different valence band arrangement between AlN and GaN, which will lead to the lower surface light extraction efficiency for the c-axis grown LED structure.[5,6] Thus, the improvement of TE polarized emission by QW structure designs is important to enhance the light extraction efficiency.

In addition, the type-II QW structure can also be expected to improve the emission efficiency due to the reduction of the effective well width and the enhancement of the optical matrix element, as reported in the literatures.[7,8] However, most research work is focused on the visible light regime, such as the type-II InGaN/GaNSb QW structure.[8] In this paper, we investigate the optical properties of the type-II InAlN-AlGaN QW structures with various In-contents in the deep-ultraviolet region. Previous study has reported that the band lineup of the InAlN/AlGaN heterojunction may be switched from type-I lineup to type-II lineup in the certain range of In-content.[9] Therefore, the type-II lineup structure may be obtained by a reasonable design.

In this study, we first calculate the valence band offset (VBO) and conduction band offset (CBO) for the $In_xAl_{1-x}N/Al_{0.59}Ga_{0.41}N$ heterojunction with various In-contents by the linear interpolation method. Then, TE/TM polarization spontaneous emission spectra of the $In_xAl_{1-x}N$–$Al_{0.59}Ga_{0.41}N/Al_{0.74}Ga_{0.26}N$ QW structures are analyzed by studying the optical matrix elements and distribution of carriers. Finally, the polarization ratios versus peak wavelength are shown for the type-II QW structures. In the calculation, the band structures and corresponding wave functions are obtained by solving the Schrödinger–Poisson equations self-consistently.[10]

2. Calculation procedures

In the calculation, the Schrödinger equation is solved by using the effective-mass theory. For obtaining the band struc-

*Project supported by the Talent Introduction Project of Nantong University, China (Grant No. 03081055), the National Natural Science Foundation of China (Grant Nos. 61874168 and 61505090), Top-notch Academic Programs Project of Jiangsu Higher Education Institutions, China (Grant No. PPZY2015B135), the Six Top Talents of Jiangsu Province, China (Grant No. 2016-XCL-052), the Natural Science Foundation of Nantong University, China (Grant Nos. 03080666 and 14Z003), the Qing Lan Project of Jiangsu Province, China, and Key NSF Program of Jiangsu Provincial Department of Education, China (Grant No. 15KJA510004).

†Corresponding author. E-mail: ntyouhua@ntu.edu.cn

© 2019 Chinese Physical Society and IOP Publishing Ltd

tures and wave functions, the block-diagonalized Hamiltonian matrix ($H^{\rm v}$) for the valence band and the single band effective mass Hamiltonian ($H^{\rm c}$) for the conduction band are adopted, which can be respectively expressed as[10–12]

$$H^{\rm v} = \begin{pmatrix} H^{\rm U} & 0 \\ 0 & H^{\rm L} \end{pmatrix}, \tag{1}$$

$$H^{\rm c}(k_{\rm t}, -{\rm i}\frac{\partial}{\partial z}) = \frac{\hbar^2}{2}\left(\frac{k_{\rm t}^2}{m_{\rm e}^{\rm t}} + \frac{-1}{m_{\rm e}^{z}}\frac{\partial^2}{\partial z^2}\right) + \Delta_1 + \Delta_2 + E_{\rm g} + P_{\rm c\varepsilon} + V_{\rm e}(z). \tag{2}$$

Here, $H^{\rm U}$ and $H^{\rm L}$ are the 3×3 upper and lower Hamiltonians. The $k_{\rm t}$ is the in-plane wave vector. The $V_{\rm e}(z)$ is the sum of the exchange–correlation energy, the band discontinuity, and the Coulomb potential energy.[13] The VBO of $In_xAl_yGa_{1-x-y}N/In_{x_0}Al_{y_0}Ga_{1-x_0-y_0}N$ is calculated by the linear interpolation method, which can be expressed as VBO $= (x-x_0)\times{\rm VBO}_{\rm InN/GaN} + (y-y_0)\times{\rm VBO}_{\rm AlN/GaN}$. ${\rm VBO}_{\rm InN/GaN}$ and ${\rm VBO}_{\rm AlN/GaN}$ denote the valence band offsets of InN/GaN and AlN/GaN, set as 0.62 eV and −0.82 eV, respectively.[14,15] The Coulomb potential energy is obtained by solving the Poisson equation in the whole region of LED, while the Schrödinger equation is only solved in the active region. In the calculation, the finite difference method is adopted with a 1 Å interval.[12] In addition, the difference of quasi Fermi levels of electrons and holes is employed as an input parameter.[10] The corresponding material parameters have been introduced in Ref. [16].

After obtaining the band structures and wave functions, the spontaneous emission rate ($r^{\rm spon}$) can be calculated as follows:[16]

$$r^{\rm spon}(\hbar\omega) = \frac{8\pi n_{\rm r}^2\hbar^2\omega^2}{h^3c^2}C_0\frac{2}{L_z}\sum_{\sigma}\sum_{n,m}\int_0^{\infty}\frac{k_{\rm t}{\rm d}k_{\rm t}}{2\pi}M_{nm}^{\sigma}(k_{\rm t})f_{\rm c}^{n} \times(1-f_{\rm v}^{\sigma m})\frac{\Gamma/\pi}{[E_{\sigma,nm}^{\rm cv}(k_{\rm t})-\hbar\omega]^2+\Gamma^2}, \tag{3}$$

$$C_0 = \frac{\pi e^2}{n_{\rm r}c\varepsilon_0 m_{\rm o}^2\omega}, \tag{4}$$

where $M_{nm}^{\sigma}(k_{\rm t})$ denotes the optical momentum matrix element for the transition between the n-th conduction sub-band and m-th valence sub-band.[17] The index σ denotes the 3×3 upper or lower Hamiltonian.

3. Results and discussion

The investigated $In_xAl_{1-x}N$–$Al_{0.59}Ga_{0.41}N/Al_{0.74}Ga_{0.26}N$ single quantum well (SQW) structure, as shown in the inset of Fig. 1(a), is consist of an n-$Al_{0.74}Ga_{0.26}N$ layer, an $In_xAl_{1-x}N$–$Al_{0.59}Ga_{0.41}N/Al_{0.74}Ga_{0.26}N$ QW layer, and a p-$Al_{0.74}Ga_{0.26}N$ layer. The well layer includes a 1 nm $In_xAl_{1-x}N$ layer and a 1 nm $Al_{0.59}Ga_{0.41}N$ layer. The barrier layer is a 10 nm $Al_{0.74}Ga_{0.26}N$ layer. The carrier concentrations of the n- and p-type layers are set as 1.78×10^{18} cm^{-3} and 1.18×10^{17} cm^{-3}, respectively, which are basically in the range reported in Ref. [18]. The Auger coefficient and the Shockley–Read–Hall (SRH) recombination lifetime are respectively set as 5×10^{-30} cm^6/s and 10 ns.[19] Figure 1(a) shows the calculated valence band offsets and conduction band offsets of $In_xAl_{1-x}N/Al_{0.59}Ga_{0.41}N$ with various In-contents. From the figure, it can be observed that a type-II lineup structure occurs in the indium-content range of ∼ 0.132–0.235. In this indium-content range, the valence band-edge and conduction band-edge of $In_xAl_{1-x}N$ are both lower than that of $Al_{0.59}Ga_{0.41}N$, as shown in Fig. 1(b).

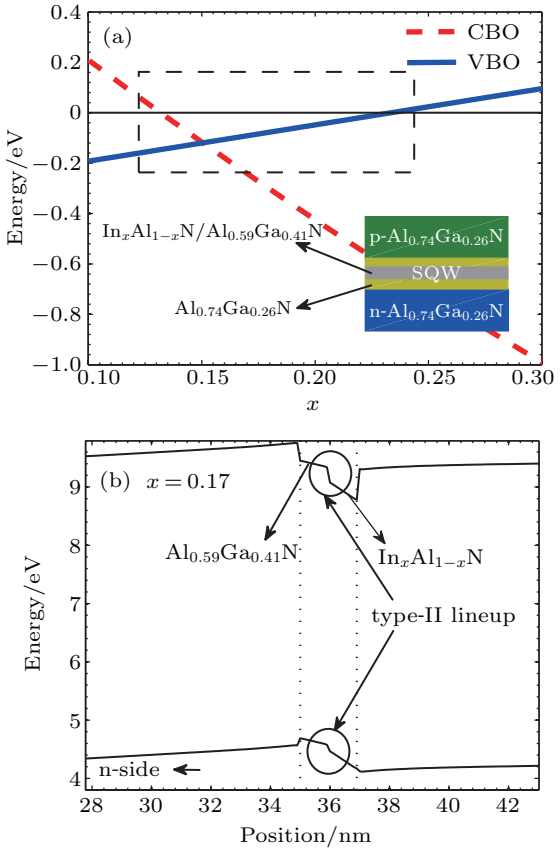


Fig. 1. (a) The calculated valence band offsets and conduction band offsets of $In_xAl_{1-x}N/Al_{0.59}Ga_{0.41}N$ and (b) the potential profile of the $In_xAl_{1-x}N$–$Al_{0.59}Ga_{0.41}N/Al_{0.74}Ga_{0.26}N$ single quantum well structure. The single quantum well structure is shown in the inset.

Figure 2 shows the TE polarization and TM polarization spontaneous emission spectra of the $In_xAl_{1-x}N$–$Al_{0.59}Ga_{0.41}N/Al_{0.74}Ga_{0.26}N$ QW structures with various In-contents at the injection current density of 100 A/cm^2. For comparison, the spectra of the conventional $Al_{0.59}Ga_{0.41}N/Al_{0.74}Ga_{0.26}N$ QW structure are also shown. In order to make the thickness of the well layer of both structures equal, the thickness of the $Al_{0.59}Ga_{0.41}N$ well layer is set as 2 nm. For the $In_xAl_{1-x}N$–$Al_{0.59}Ga_{0.41}N/Al_{0.74}Ga_{0.26}N$ QW structures, the peak intensities in the spontaneous emission spectrum of TE mode are increased by 47.45%–53.84% as compared to those of the conventional structure. The largest

TE mode peak intensity is obtained in the type-II QW structure with $x \sim 0.17$, which is basically consistent with the experimental result reported in Ref. [9]. Moreover, it is also observed that the TM polarization spontaneous emission rate of the $In_xAl_{1-x}N$–$Al_{0.59}Ga_{0.41}N/Al_{0.74}Ga_{0.26}N$ QW structures is obviously smaller than that of the conventional structure. In order to explain these phenomena, we calculate the optical matrix elements and the carrier distribution.

Figures 3(a) and 3(b) show the optical matrix elements as a function of the in-plane wave vector k_t for the $In_{0.15}Al_{0.85}N$–$Al_{0.59}Ga_{0.41}N/Al_{0.74}Ga_{0.26}N$ QW structure and the conventional $Al_{0.59}Ga_{0.41}N/Al_{0.74}Ga_{0.26}N$ QW structure, where c1 is the lowest conduction sub-band and v1, v2, and v3 are the top three valence sub-bands. Note that v1–v3 are obtained by using the upper Hamiltonian. For the c1–v1 transition, the TE polarization optical matrix elements ($|M_x|^2$) of both structures are almost the same. However, for the c1–v2 and c1–v3 transitions, the $|M_x|^2$ of the conventional structure is far larger than that of the $In_{0.15}Al_{0.85}N$–$Al_{0.59}Ga_{0.41}N/Al_{0.74}Ga_{0.26}N$ QW structure in the vicinity of the Γ point. In addition, the TM polarization optical matrix elements ($|M_z|^2$) of the conventional structure for these transitions are also larger, especially for the c1–v1 transition. Figure 3(c) shows the product of the Fermi–Dirac distribution functions of electron (f_c^n) and hole $(1 - f_v^{Um})$. It can be seen that the product $f_c^n(1 - f_v^{Um})$ of the type-II QW structure is larger than that of the conventional QW structure for the c1–v1, c1–v2, and c1–v3 transitions. According to formula (4), the spontaneous emission rate is proportional to the optical matrix element and $f_c^n(1 - f_v^{Um})$. Thus, the larger peak intensity in the TE polarization spontaneous emission spectrum for the type-II lineup structure can be attributed to the larger product of $f_c^n(1 - f_v^{Um})$ and the approximately equal $|M_x|^2$ for the c1–v1 transition. Meanwhile, the larger TM polarization peak intensity of the conventional structure can be mainly attributed to the larger $|M_z|^2$ for the c1–v1 transition.

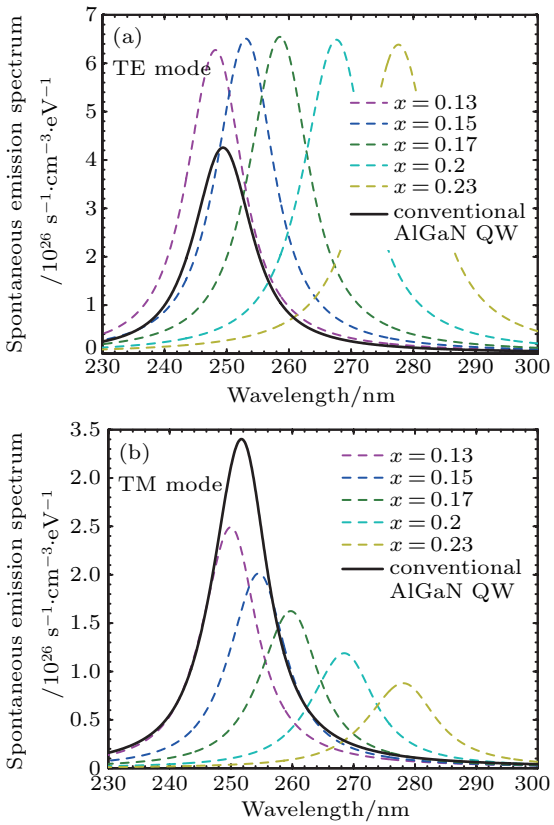


Fig. 2. (a) TE polarization and (b) TM polarization spontaneous emission spectra of the $In_xAl_{1-x}N$–$Al_{0.59}Ga_{0.41}N/Al_{0.74}Ga_{0.26}N$ QW structures and the conventional $Al_{0.59}Ga_{0.41}N/Al_{0.74}Ga_{0.26}N$ QW structure at the injection current density of 100 A/cm^2.

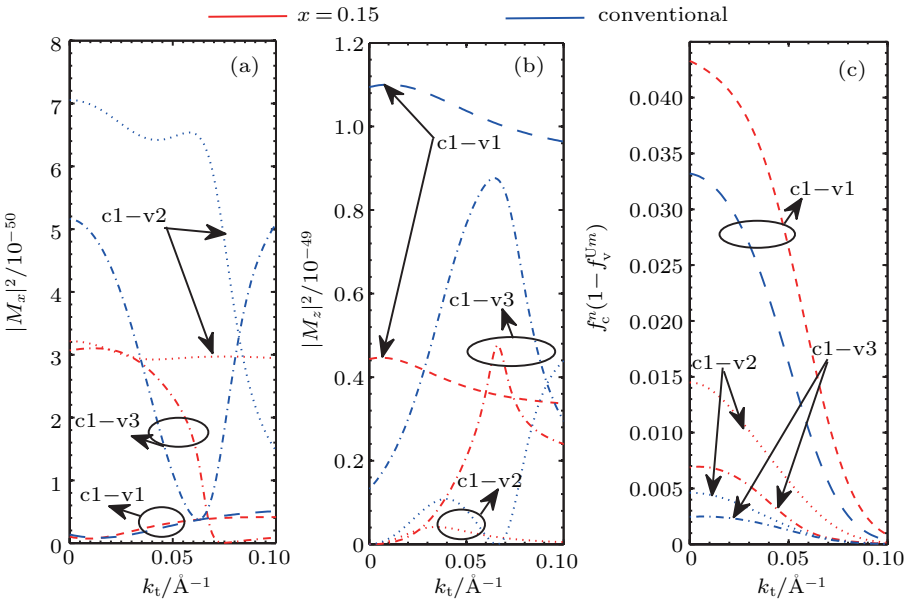


Fig. 3. (a) TE-polarized optical matrix elements ($|M_x|^2$), (b) TM-polarized optical matrix elements ($|M_z|^2$), and (c) the product of Fermi–Dirac distribution functions of electron and hole as a function of the in-plane wave vector k_t for the $In_{0.15}Al_{0.85}N$–$Al_{0.59}Ga_{0.41}N/Al_{0.74}Ga_{0.26}N$ QW structure and the conventional structure.

Figure 4 shows the TE-polarized and TM-polarized optical matrix elements and $f_c^n(1-f_v^{Um})$ at the Γ point for the $In_xAl_{1-x}N$–$Al_{0.59}Ga_{0.41}N/Al_{0.74}Ga_{0.26}N$ QW structures with different In-contents. From Fig. 4(a), it can be observed that the TE-polarized optical matrix element with increasing the In-content firstly decreases slightly and then increases for the c1–v1 transition, and $|M_x|^2$ decreases for the c1–v2 and c1–v3 transitions. Moreover, the $|M_x|^2$ for the c1–v1 transition is far smaller than that for the c1–v2 and c1–v3 transitions. However, for $f_c^n(1-f_v^{Um})$, the trend is completely opposite as shown in Fig. 4(c). Thus, the change of the peak intensity for the TE mode with In-content as shown in Fig. 2(a) can be attributed to the combined effect of $|M_x|^2$ and $f_c^n(1-f_v^{Um})$ for these transitions. For the TM polarization, the optical matrix element for the c1–v1 transition is much larger as compared to that for the c1–v2 and c1–v3 transitions as shown in Fig. 4(b). And $|M_z|^2$ for the c1–v1 transition decreases with increasing In-content, which will lead to the reduction of the TM polarization spontaneous emission rate. Thus, the change of the TM polarization spontaneous emission rate with In-content can be mainly attributed to the reduction of $|M_z|^2$ for the c1–v1 transition.

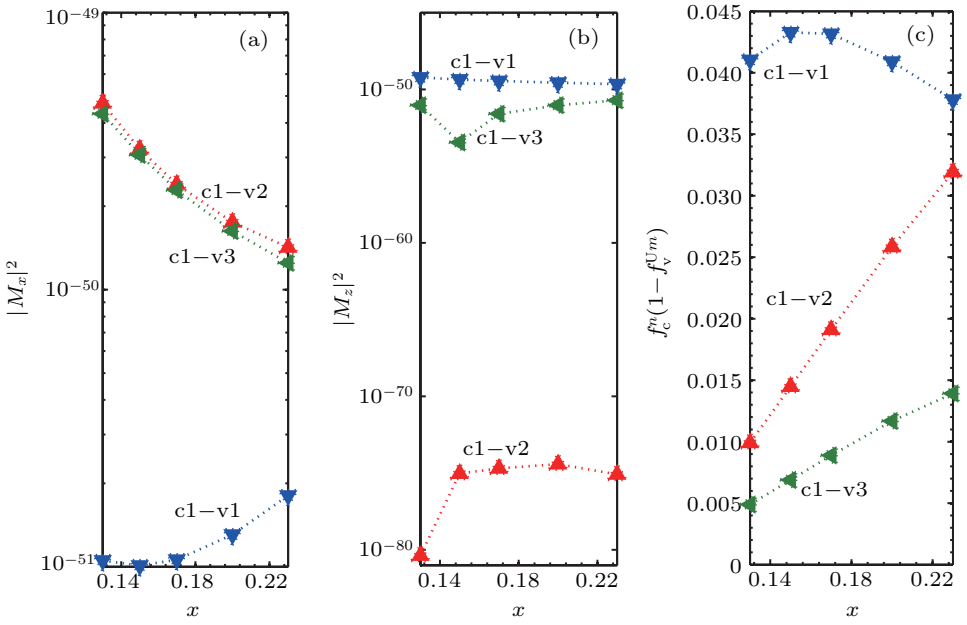


Fig. 4. (a) TE-polarized and (b) TM-polarized optical matrix elements and (c) $f_c^n(1-f_v^{Um})$ at the Γ point for the $In_xAl_{1-x}N$–$Al_{0.59}Ga_{0.41}N/Al_{0.74}Ga_{0.26}N$ QW structures with different In-contents.

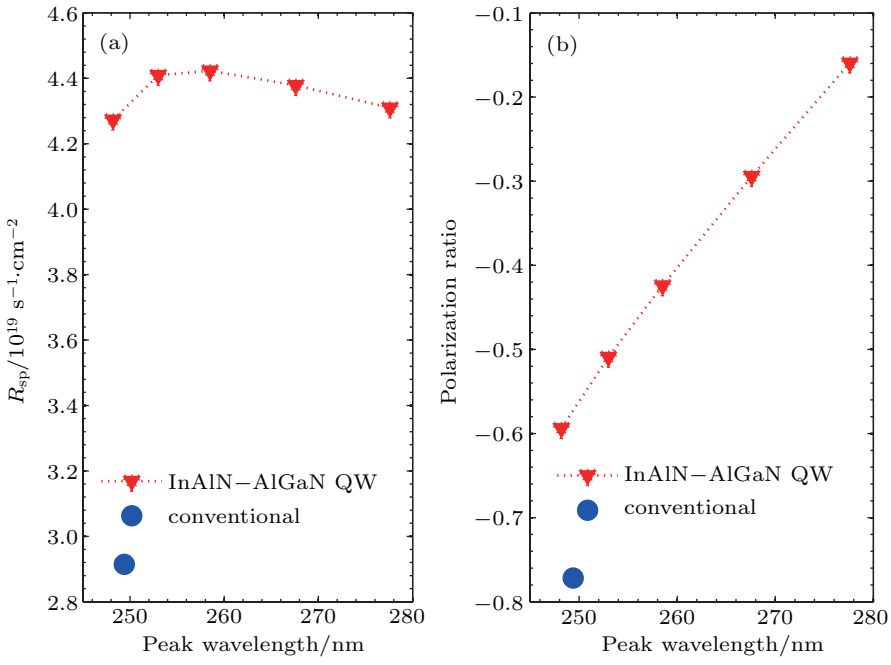


Fig. 5. (a) The TE polarization total spontaneous emission rate (R_{sp}) and (b) polarization ratio as a function of peak wavelength for the $In_xAl_{1-x}N$–AlGaN/$Al_{0.74}Ga_{0.26}N$ QW structures ($x = 0.13, 0.15, 0.17, 0.2, 0.23$) and the conventional structure at the current density of 100 A/cm^2.

Finally, one shows the TE polarization total spontaneous emission rate (R_{sp}) and the polarization ratio as a function of peak wavelength of the $In_xAl_{1-x}N$–AlGaN/$Al_{0.74}Ga_{0.26}N$ QW structures ($x = 0.13, 0.15, 0.17, 0.2, 0.23$) and the conventional structure at the current density of 100 A/cm^2 in Fig. 5. The polarization ratio is defined as $(I_{TE} - I_{TM})/(I_{TE} + I_{TM})$.[20] Here, I_{TE} and I_{TM} denote the TE-polarized R_{sp} and TM-polarized R_{sp}. The total spontaneous emission rate can be obtained by the formula $R_{sp} = L_z \int_0^\infty r^{spon}(\hbar\omega)\mathrm{d}\hbar\omega$. It can be seen that the TE-polarized R_{sp} of the $In_xAl_{1-x}N$–AlGaN/$Al_{0.74}Ga_{0.26}N$ QW structures first increases and then decreases with increasing the In-contents due to the combined effect of $|M_x|^2$ and $f_c^n(1 - f_v^{Um})$ as discussed above. In addition, the absolute value of polarization ratio for the conventional structure is much larger than that for the $In_xAl_{1-x}N$-AlGaN/$Al_{0.74}Ga_{0.26}N$ QW structures, which indicates the strong TM mode emission. By replacing the AlGaN well layer with $In_xAl_{1-x}N$–AlGaN layer, the degree of polarization of the DUV LEDs can be much reduced and TE polarized emission can be significantly enhanced.

4. Conclusion

In summary, we have investigated the optical properties of the type-II lineup $In_xAl_{1-x}N$–$Al_{0.59}Ga_{0.41}N$/$Al_{0.74}Ga_{0.26}N$ QW structures with various In-contents by using the effective mass theory. As compared to the conventional structure, the type-II lineup structure has much larger TE polarization spontaneous emission rate due to the larger product of $f_c^n(1 - f_v^{Um})$ and the approximately equal $|M_x|^2$ for the c1–v1 transition. In addition, the TE-polarized R_{sp} of the $In_xAl_{1-x}N$-AlGaN/$Al_{0.74}Ga_{0.26}N$ QW structures has a maximal value in the range of $x = 0.13$–0.23 at the injection current density of 100 A/cm^2. It can be attributed to the combined effect of $|M_x|^2$ and $f_c^n(1 - f_v^{Um})$ for the c1–v1, c1–v2, and c1–v3 transitions.

References

[1] Hirayama H, Fujikawa S and Kamata N 2015 *Electron. Commun. Jpn.* **98** 1

[2] Liu C, Ooi Y K, Islam S, Xing H, Jena D and Zhang J 2018 *Appl. Phys. Lett.* **112** 011101

[3] Wang L, Song W, Hu W, Li G, Luo X, Wang H, Xiao J, Guo J, Wang X, Hao R, Yi H, Wu Q and Li S 2019 *Chin. Phys. B* **28** 018503

[4] Hideki H, Yusuke T, Tetsutoshi M and Norihiko K 2010 *Appl. Phys. Express* **3** 031002

[5] Jiang X, Shi J, Zhang M, Zhong H, Huang P, Ding Y, Yu T, Shen B, Lu J and Wang X 2014 *New J. Phys.* **16** 113065

[6] Su C Y, Tsai M C, Chou K P, Chiang H C, Lin H H, Su M Y, Wu Y R, Kiang Y W and Yang C C 2017 *Opt. Express* **25** 26365

[7] Arif R A, Zhao H P and Tansu N 2008 *Appl. Phys. Lett.* **92** 011104

[8] Park S H, Ahn D, Koo B H and Oh J E 2010 *Appl. Phys. Lett.* **96** 051106

[9] Zubialevich V Z, Alam S N, Li H N and Parbrook P J 2016 *J. Phys. D: Appl. Phys.* **49** 385105

[10] Wenzel H 2007 *Opt. Quant. Electron.* **38** 953

[11] Chuang S L and Chang C S 1996 *Phys. Rev. B* **54** 2491

[12] Chuang S L and Chang C S 1997 *Semicond. Sci. Tech.* **12** 252

[13] Vurgaftman I and Meyer J R 2007 *Nitride Semiconductor Devices: Principles and Simulation* (Gemany: Wiley-VCH Verlag GmbH & Co. KGaA) pp. 121, 309

[14] Moses P G and Van de Walle C G 2010 *Appl. Phys. Lett.* **96** 021908

[15] Li H, Liu X, Sang L, Wang J, Jin D, Zhang H, Yang S, Liu S, Mao W, Hao Y, Zhu Q and Wang Z 2014 *Phys. Status. Solidi. B* **251** 788

[16] Li Y, Zhu Y, Huang J, Deng H, Wang M and Yin H 2017 *J. Appl. Phys.* **121** 053105

[17] Li Y, Zhang R, Xie Z, Liu B, Chen P, Zhang G, Tao T, Zhuang Z, Zhi L, Gan T and Zheng Y 2013 *J. Appl. Phys.* **114** 113104

[18] Wang J, Yan J, Guo Y, Zhang Y, Tian Y, Zhu S, Chen X, Sun L and Li J 2015 *Sci. Sin. Phys. Mech. & Astron.* **45** 067303-067301-067303

[19] Kuo Y K, Chang J Y, Chang H T, Chen F M, Shih Y H and Liou B T 2017 *IEEE J. Quantum Elect.* **53** 1

[20] Zhuang Z, Li Y, Liu B, Guo X, Dai J, Zhang G, Tao T, Zhi T, Xie Z, Ge H, Shi Y, Zheng Y and Zhang R 2015 *J. Appl. Phys.* **118** 233111